Feed Forward Control of *L*-Methionine Using Sequential Adaptive Networks

Rajib Nayak and James Gomes
Department of Biochemical Engineering and Biotechnology, Indian Institute of Technology, New Delhi, India, 110016
rajib.nayak@gmail.com, gomes@dbeb.iitd.ernet.in

Abstract

The objective of this work is to study the performance of a feed forward controller that incorporates Sequential Adaptive Networks (SAN) for controlling the methionine concentration of fed-batch fermentation process along a predefined trajectory. A feed forward control law is formulated using a mechanistic model for the process. SAN is an assembly of chronologically ordered networks with one sub network assigned to each sampling interval. SAN can be used to predict the measured and unmeasured states of the process at one time step ahead. An actual process scenario is created by incorporating noise in dissolved oxygen (DO) concentration measurements and allowing the parameters of the mechanistic model to vary with time. The difference between the measured values of DO with the values predicted by SAN is used to update the weights of the SAN at each sampling time interval. The performance of SAN-feed forward controller exhibits precise prediction of unmeasured states and a robust and stable tracking of the methionine concentration trajectory.

1. Introduction

Hybrid Modeling has been used effectively to design control strategies for bioprocesses [1-8]. A hybrid model is usually a combination of a mechanistic (white box) model and a neural network (black box) model. It brings together the relative advantages of the different model types. The mechanistic component is based on physical phenomena and provides a means of data interpretation. The black box component circumvents the difficulties of modeling complex behavior and act as virtual sensors for variables that cannot be measured physically. One such application in controlling methionine production in a fed-batch process is presented here.

Methionine synthesis within a microorganism is strictly regulated at the gene and enzyme level because it is energy intensive and it occurs at the terminal end of the metabolic pathway of the aspartic family of amino acids. It is one of the only two sulfur containing amino acid and plays a critical role in protein synthesis. Consequently, the time profile of methionine concentration in fed-batch processes exhibits strong nonlinear characteristics. There are no sensors for measuring methionine online. The measurement of the cell and substrate concentrations is beset with several practical problems such as the blockage of sampling lines. On the other hand, the dissolved oxygen (*DO*) concentration can be measured accurately and quickly. Further, oxygen being one of the terminal electron acceptors in aerobic growth, it reflects the metabolic (physiological) state of the process. We have developed a new mechanistic model to describe the intrinsic kinetics of methionine production. A feed forward controller is derived from this model and it is used in conjunction with Sequential Adaptive Networks (SAN) to control methionine synthesis along a desired linear trajectory.

In this paper, we present the development of the feed forward controller and its integration with SAN for controlling methionine production. The feed forward control law is derived from the dynamic equations of the mechanistic model. The control action is computed based on the prediction of states determined using SAN. The difference between the predicted and measured values of *DO* concentration is used for on-line adaptation of SAN to the changing physiological conditions. The performance of the SAN-feed forward controller is studied for the cases when process parameters are time varying and *DO*

measurements contain noise. The results are presented and discussed.

2. Theoretical development

2.1 SAN architecture and adaptation algorithm

Reactor conditions influence the physiological state of the cell population. These conditions are manipulated primarily by changing nutrient feed rates and oxygen supply rates. The degree of influence of reactor conditions on the cells also depends on whether the cells are in the growth phase or production phase. Hence the response of the cells to external manipulation is complex. It is difficult to capture all the features of the response dynamics using a single neural network. A single neural network is more effective in predicting the more recent training data and less effective in predicting past trends. To address this problem, SAN architecture was constructed. SAN is an assembly of neural networks with each sub-network being assigned to a sampling interval in a chronological order. Each sub-network captures the various physiological states occurring within its assigned time frame. Each of these networks in turn is adapted to changing process conditions based on on-line measurement that guide the entire ensemble along the evolution of the process. Consequently, during recall and generalization, SAN has the flexibility to move from one physiological pattern to another across the sequence of sub-networks.

In this study, each of the sub-networks is identical. The connections between the layers of different nodes are of the feed forward type. The process variables s, x, c_l, p, V (glucose, biomass, DO, methionine concentrations and volume of reactor, respectively), and process parameters m and s_f (desired rate of methionine production and substrate concentration in feed, respectively) are inputs to each of the sub-networks. The output variables of each sub-network are s, x, c_l, p and V predicted one time step ahead. Further, there are intra-connections from DO nodes to other nodes in output layer for adaptation with changing process dynamics.

The mathematical formulation is described by the following equations. Considering the hidden layer input (H_j in) and output (H_j out), we obtain the relations

$$H_j in = \sum_i U_{ij} I_i + \xi_j \tag{1}$$

$$H_j out = \phi(H_j in) \tag{2}$$

Considering the output layer input (O_k in) and output (O_k out), we obtain the relations

$$O_k in = \sum_j V_{jk} H_j out + W_k O_{DO} out(n-1) + \xi_k \tag{3}$$

$$H_j out = \phi(H_j in) \tag{4}$$

Error with respect to the desired values is given by

$$e_k = d_k - \mathrm{O_k} out \tag{5}$$

and the total mean square error (m^{th} dataset, for the particular sampling interval)

$$E_m = \frac{1}{2} \sum_k e_k^{\,2} \tag{6}$$

Total error of m datasets is therefore

$$E = \sum_m E_m \tag{7}$$

The weights are updated as follows

$$\Delta W_k = -\eta \frac{\partial E_m}{\partial W_k} + \alpha\left(\Delta W_k(n-1)\right) \tag{8}$$

$$W_k(n) = W_k(n-1) + \Delta W_k \tag{9}$$

$$\Delta V_{jk}(n) = -\eta \frac{\partial E_m}{\partial V_{jk}} + \alpha\left(\Delta V_{jk}(n-1)\right) \tag{10}$$

$$V_{jk}(n) = V_{jk}(n-1) + \Delta V_{jk}(n) \tag{11}$$

$$\Delta U_{ij}(n) = -\eta \frac{\partial E_m}{\partial U_{ij}} + \alpha\left(\Delta U_{ij}(n-1)\right) \tag{12}$$

$$U_{ij}(n) = U_{ij}(n-1) + \Delta U_{ij}(n) \tag{13}$$

Where, U_{ij}, V_{jk} and W_k are the weights between input and hidden layer, hidden and output layer and intra-connections in output layer respectively. d_k is the desired output. I_i is the input to the networks. The activation function ϕ for input to hidden layer is a tan hyperbolic function, and activation function Ψ for hidden layer to output layer is a positive sigmoidal function. The bias is shown as ξ; α is the momentum coefficient and η is the learning rate.

For implementing the SAN-FF controller online, the trained and generalized network is employed. As the process conditions begin to change and move away from the training regime, the weights need to be adapted based on online process measurements. We used the online *DO* measurements and its deviation from the prediction of SAN to adapt the weights in real time. The error equation becomes

$$e_{k,online} = d_{k,DO\,online} - O_k out \qquad (14)$$

Equations (6) to (13) are recomputed at every sampling interval so that the weights are continuously adapted to the dynamic behavior of the process. Since the SAN is pre-trained, the adaptation of parameters is completed within average time of about 15 sec.

The training for SAN has been described with the help of Fig 1. For any sampling instant $\Delta t = t_n - t_{n-1}$, the sub-network is presented with data for that time interval alone during entire training procedure. The data for different experiments are presented in sequence to the sub-networks in strict chronology until generalization is achieved. Thus, for the composite SAN, one cycle of training completes when the errors are below the acceptable limit for the entire network. However, for each sub-network, the cycle of training completes when all 32 experimental data sets have been presented to SAN. Hence, in Fig 1, the generalization is indicated in the chronological direction, whereas the training of the sub-networks is shown in the perpendicular direction of presentation of the experimental data sets.

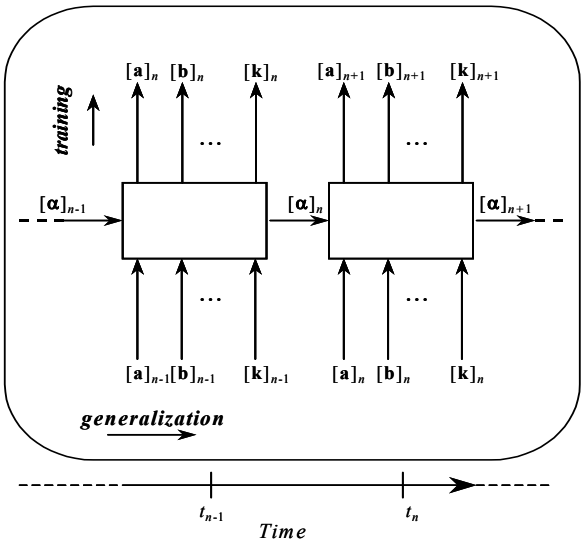

Figure 1: Architecture of SAN

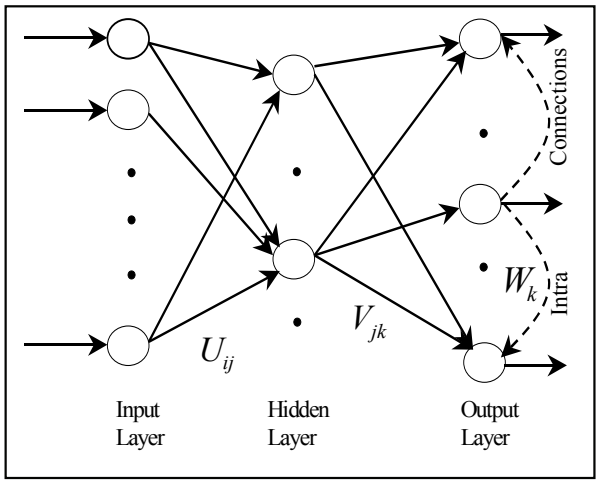

Figure 2: Schematic diagram of feed-forward neural network for each sub-network of SAN

2.2 Fed-batch model for methionine production

In the absence of large experimental data sets, the mechanistic model developed was used to generate the data required for training the SAN. The mechanistic model incorporates an exponential term to describe the prolonged lag phase and the rapid changes to environmental which is not possible with the Monod structure. A metabolic switching function (Eq. 21) was used to describe the change in metabolism that occurs with the changing *DO* concentration in the reactor. The second trigger (Eq. 17) was used to describe the re-utilization of methionine when the substrate concentration drops below a critical value in the external environment. These features enable an accurate prediction of methionine production in a fed-batch reactor. The equations for fed-batch methionine production model are

$$\frac{dx}{dt} = \left(f(c_l)\mu(s) - D\right)x \qquad (15)$$

$$\frac{ds}{dt} = -\left[\xi_1 f(c_l)\mu(s)x + \xi_2 x\right] + D\left(s_f - s\right) \qquad (16)$$

$$\frac{dp}{dt} = \left[\alpha\frac{\left(s - s_c\right)}{s}px + \beta f(c_l)\mu(s)x\right] - Dp \qquad (17)$$

$$\frac{dc_l}{dt} = \left[K_l a\left(c_l^* - c_l\right) - \left\{\kappa\mu(s)f(c_l) + \lambda\right\}x\right] \qquad (18)$$

$$\frac{dV}{dt} = F(t) \qquad (19)$$

$$\mu(s) = \mu_m \exp(-K_e / s)\exp(-s / K_i) \qquad (20)$$

$$f(c_l) = \frac{(c_l/0.008)^6}{(0.0032/0.008)^6 + (c_l/0.008)^6} \quad (21)$$

Where x, s, c_l, p are the biomass, substrate, DO and methionine concentration (g l^{-1}) respectively. D is the dilution rate (h^{-1}), t is the time (h), s_f is the substrate concentration in the feed (g l^{-1}) and V is the volume of the reactor (l). The values and description of the model parameters are given in the Appendix.

2.3 Development of control strategy

There are several experimental observations that are accounted for in the development of the feed forward control law for methionine production. The substrate (glucose) is consumed rapidly and reaches a critical value at the later part of the batch process of methionine production. The methionine is re-utilized by the microorganism to maintain an energy economy when the substrate falls below a critical value (s_c). Further, the specific growth rate and the rate of methionine production are strongly influenced by oxygen; both these rates are near their maximum values when the *DO* concentration is about 40%.

The purpose of the control strategy is to maintain the rate of production of methionine at its maximum throughout the fed-batch process. From the experimental data [9, 10] the rate is constant just before it reaches the critical concentration s_c. Consequently, the desired profile is a simple linear equation.

$$p = p_0 + mt \quad (22)$$

Where p_0 is methionine concentration at the end of the batch phase and m is the desired rate of methionine production in the fed-batch phase. Since the oxygen concentration is measured with the standard modules of reactors, the on-line measurements of *DO* concentrations is used the SAN-feed forward controller. The SAN is used to predict the measured and unmeasured state variables that are required to calculate the control variable and for on-line adaptation to the changing process conditions. The controller output, the substrate feed flow rate (F), is calculated from the feed forward law one sampling time ahead. The feed forward law is designed to give the value of feed rate such that the substrate added to reactor keeps the residual substrate concentration above the critical value and the methionine concentration along the desired linear profile.

Now from equation (17) and (22) we can calculate D and hence the substrate feed rate as

$$D = \frac{F}{V} = \left[\left\{\alpha \frac{(s - s_c)}{s} x\right\} + \left\{\frac{\beta\mu(s) f(c_l) x}{p}\right\}\right] - \left(\frac{m}{p}\right) \quad (23)$$

For on-line implementation, the SAN is trained on simulated data sets. The trained SAN has reasonable prediction capacity that needs to be adapted to the changing process conditions to meet the performance criteria in control implementations. At every sampling instant the weights of the individual sub-networks of the SAN are updated by minimizing the difference between the predicted and measured values of *DO* concentration. This is carried out for each sub-network sequentially. The flow diagram of control strategy is given in Fig 3.

3. Results and discussions

3.1 Generation of data sets

The model equations (15) – (21) were integrated to generate the data sets for training, validation and implementation of SAN. The data was generated at a constant sampling interval 30 min for 60 h with batch volume was 6 l. Experimental results [9, 10] suggests that available substrate is higher than the critical substrate level s_c until about 42 h. After this the residual substrate concentration falls below the critical concentration and at this point in time the SAN-feed forward controller is initiated. The reactor switches from batch mode to fed-batch mode operation at this point. Training, validation and implementation data sets were generated with three varying initial conditions, namely, substrate concentration in feed (s_f), initial substrate concentration and slope of the methionine concentration (m) with respect to time are shown in Fig 4. The data sets were chosen to span a large region of metabolic space of the process while remaining in the physical constraints, such as maximum working volume of the reactor. The filled and unfilled circles together depict the spread of data across the metabolic space. The filled circles represent the conditions used for this work while the unfilled circles are the unused conditions. The values of initial methionine concentration, initial *DO* concentration,

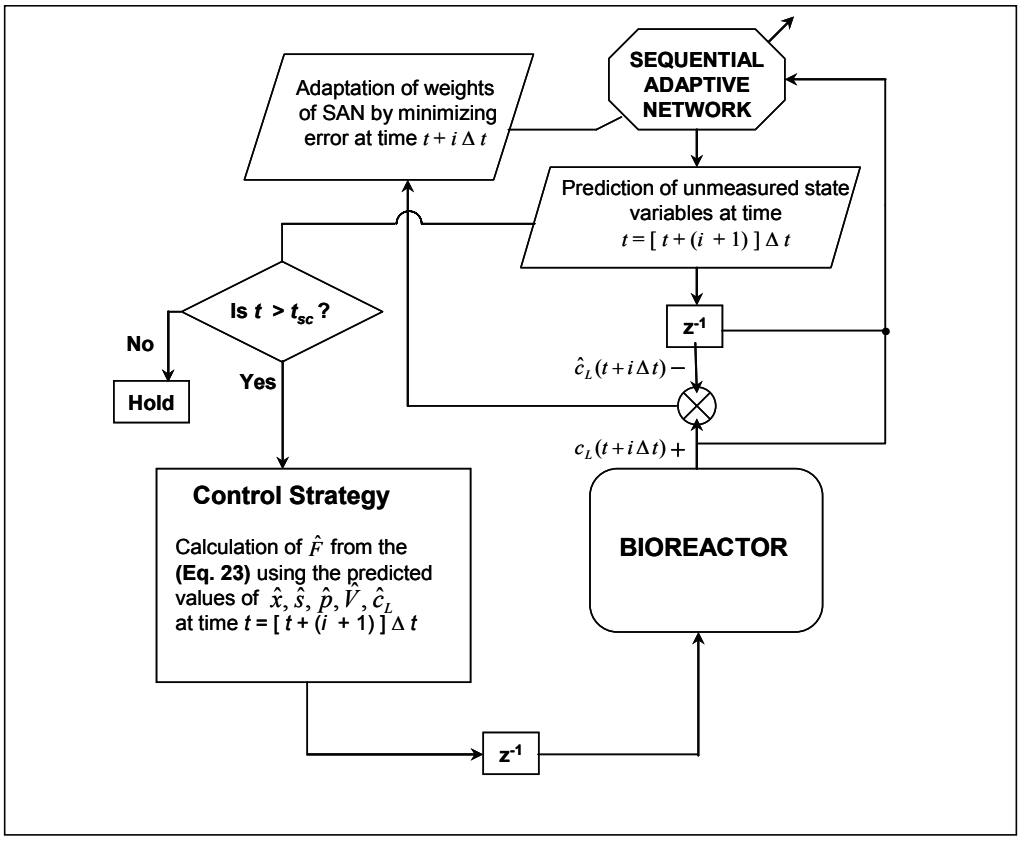

Figure 3: Flow diagram of SAN based feed forward control strategy for methionine production system

initial biomass concentration and volume of the reactor were 0.0001 gl^{-1}, 0.0032 mgl^{-1}, 1.15 gl^{-1} and 6 l respectively. The values of these initial conditions were kept constant throughout the simulation for generating data sets. Four data sets from the each corner of the cube data sets (total thirty two) were taken for training. Among seven data sets from the centre of cube, six are taken for validation and one data set is used for implementation.

3.2 Training and generalization performance of SAN

One hundred and twenty one sub-networks were employed to model the 60 h long methionine production system as each sub-network was used to monitor the 30 min sampling time interval. Initial weights were assigned randomly between -0.1 to +0.1. The number of hidden nodes was optimized with respect to recall error, the number of iteration to converge the networks and computational time required. Ten hidden nodes were found to be optimum. The final architecture 7 – 10 – 5 was used for each sub-network of SAN. The learning rate and momentum coefficient was fixed to the value 0.05 and 0.95 respectively. The methionine production process is a combination of two phases – a batch phase of 42 h followed by a fed-batch phase of 18 h. At the end of the batch phase, control is initiated to maintain the methionine along a predetermined linear trajectory (see Figs 9-11 and Fig15-16). The training data was generated for a range of metabolic conditions (Fig4) to meet these requirements. In particular, the result of point A (Fig 4: s_0 = 55 g l^{-1}, s_f = 12 g l^{-1}, m = 0.07 g l^{-1} h^{-1}) is presented here. Fig. 5 shows prediction of x, s and p and Fig. 6 shows the prediction of c_L and V after training. SAN was trained for an average threshold Root Mean Square Error (RMSE) of 10^{-5} per data point. The average number of iterations per feed forward neural network unit was 2000. Six validation points were used to check the generalization of SAN (Fig. 4). The recall profiles for point B (Fig 4: s_0 = 60

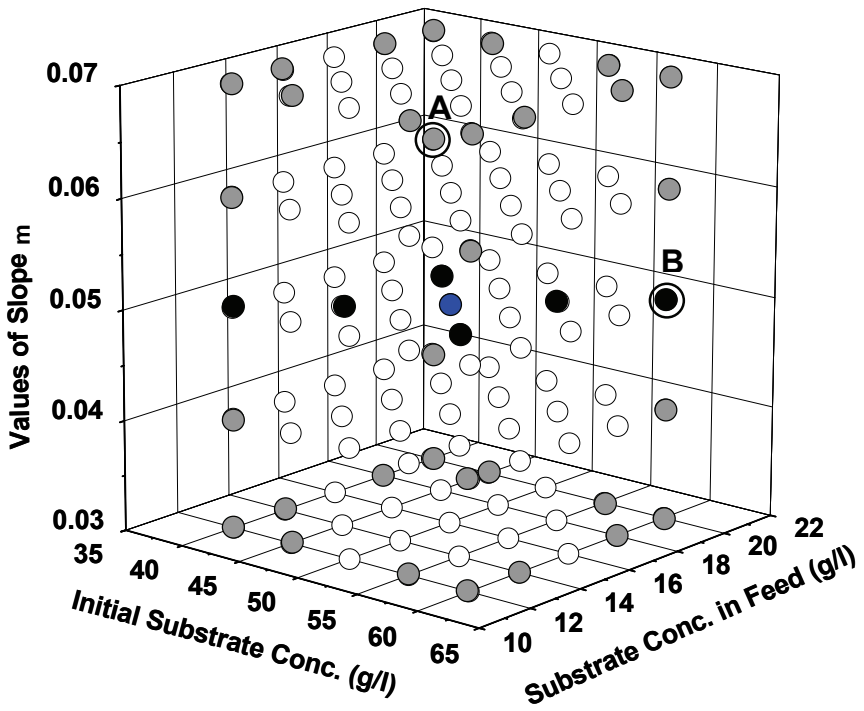

Figure 4: Various combination of initial conditions to generate data sets. The grey, black and blue colors represents for training, validation and implementation data sets; the white circles, although unused in this study, represents the range of metabolic states that the system can exhibit in the domain of interest

g l^{-1}, s_f = 20 g l^{-1}, m = 0.05 g l^{-1} h^{-1}) are shown in Figs. 7 and 8. The recall profiles matched the training data sets profiles with recall errors of the order of 10^{-5}. For validation of SAN outside the training domain, recall profiles matched the simulation profiles with generalization errors (RMSE per data points) of the order of the 10^{-3} to 10^{-4}. The NRMSE analysis of six validation data points is given in the Table 1.

3.3 Performance of SAN-feed forward controller under ideal conditions

Implementation of SAN was performed for several conditions. The result for the centre point of the cube is presented is presented here. In this case, the initial substrate concentration is 50 g l^{-1}, substrate concentration in feed is 16 g l^{-1} and slope of the methionine concentration is 0.05 g l^{-1} h^{-1}.

Table 1: NRMSE analysis of six validation data sets

Data Sets No	Varying Conditions			Total RMSE	NRMSE				
	s	s_f	m		s	x	p	V	c_l
01	45	18	0.05	9.8×10^{-4}	2.2×10^{-3}	2.1×10^{-3}	7.2×10^{-4}	3.7×10^{-3}	1.8×10^{-5}
02	55	14	0.05	1.5×10^{-3}	1.3×10^{-3}	3.6×10^{-3}	4.1×10^{-3}	4.4×10^{-3}	1.7×10^{-5}
03	45	14	0.05	6.3×10^{-4}	1.9×10^{-3}	1.4×10^{-3}	9.6×10^{-4}	1.6×10^{-3}	1.7×10^{-5}
04	40	12	0.05	9.3×10^{-4}	2.1×10^{-3}	1.5×10^{-3}	1.4×10^{-3}	3.5×10^{-3}	1.7×10^{-5}
05	55	18	0.05	5.8×10^{-4}	5.1×10^{-4}	4.6×10^{-4}	2.8×10^{-3}	2.1×10^{-3}	1.5×10^{-5}
06	60	20	0.05	3.9×10^{-4}	7.2×10^{-4}	2.4×10^{-4}	1.6×10^{-3}	7.8×10^{-4}	1.3×10^{-5}

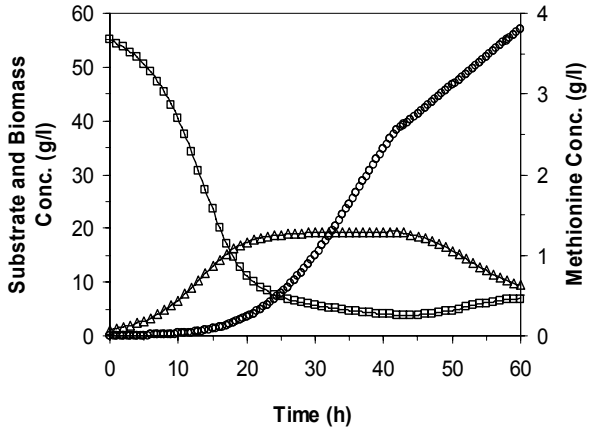

Figure 5: SAN accurately recalls the methionine, substrate and biomass concentration of training data. The SAN prediction (—) matches the training data (○ Methionine □ Substrate and Δ Biomass concentrations)

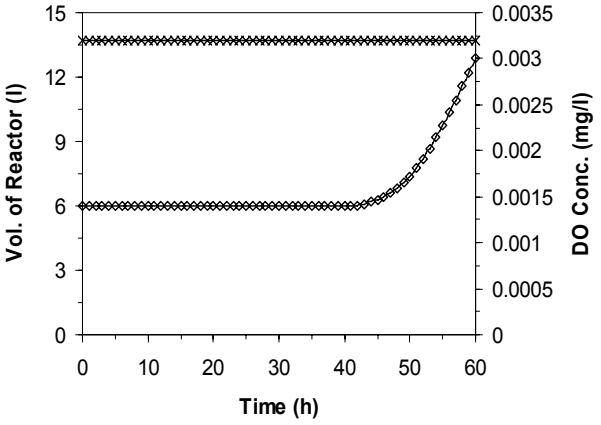

Figure 6: SAN accurately recalls the *DO* concentration and reactor volume of training data. The SAN prediction (—) matches the training data (× *DO* concentration and ◊ volume of reactor)

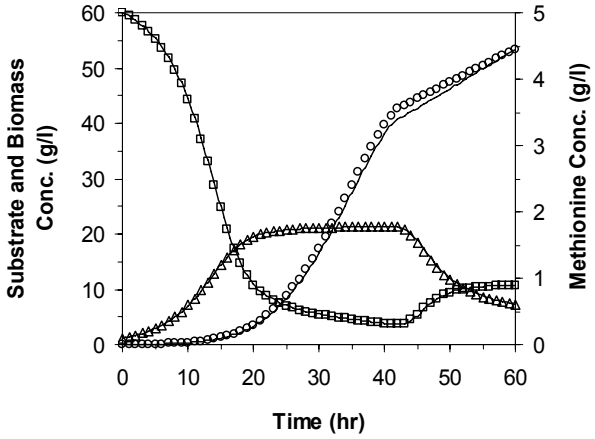

Figure 7: Validation profile of SAN for methionine, substrate and biomass concentration for a data set taken outside its training domain shows generalization. Prediction of SAN (—); Actual data (○ Methionine □ Substrate and Δ Biomass concentrations)

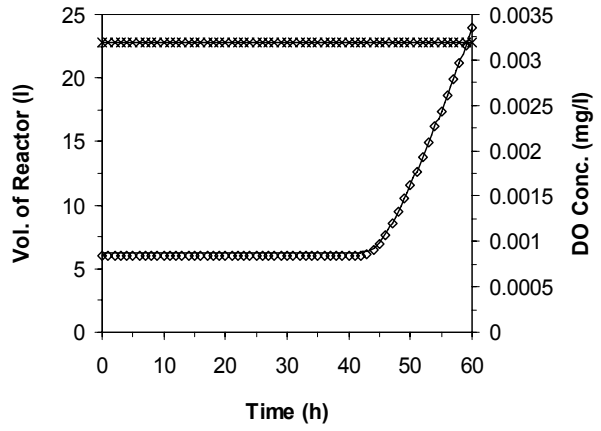

Figure 8: Validation profile of SAN for *DO* concentration and reactor volume for a data set taken outside its domain of training shows generalization. Prediction of SAN (—); Actual data (× *DO* concentration and ◊ volume of reactor)

The manipulated variable (F) was computed using the feed forward control law (Eq. 23) using the one time step ahead prediction from SAN. The weights of SAN were updated on-line using the error values between measured and predicted *DO* concentration. The methionine production profiles and the control action are shown in the Figs 9 and 10 respectively and the detailed NRMSE analysis is given in Table 2. Figure 9 shows the performance of the SAN-FFC. The control action shown in Fig. 10 is based on the prediction of SAN. The SAN-FFC acts in such a way that the methionine concentration in the reactor converges to the desired trajectory *XY* shown in Fig. 9. The control action is smooth and the desired concentration is achieved before 60 h. The computation of the control action (Eq. 23) depends on other variables besides methionine. In Eq. 23, since β is smaller than α, the under prediction of p at the

beginning of the fed batch phase does not degrade the controller performance. As the information from the actual process conditions (from *DO* measurements) is used to update the SAN, the prediction of *p* improves and finally matches that of the process. Our previous work has shown that without *DO* measurements the performance of such controllers degrades rapidly [8]. Biological systems are slow and have an intrinsic response time. This is exhibited as the gradual increase in the slope of the concentration as it meets the desired concentration trajectory.

3.4 Performance of SAN-feed forward controller in the presence of noise in DO measurement

Measurement of any process variable in actual experiments is always associated with noise. A controller should give stable and robust performance in these situations. To investigate the performance of SAN based hybrid controller for real world application, it is studied with 5% random noise was added to the on-line *DO* measurements. The initial substrate concentration was 50 g l^{-1} and the substrate feed concentration was 16 g l^{-1} as before. The simulation results are shown in Figs 11 and 12 and NRMSE analysis is given in Table 2. Figure 11 shows the prediction of three unmeasured state variables;

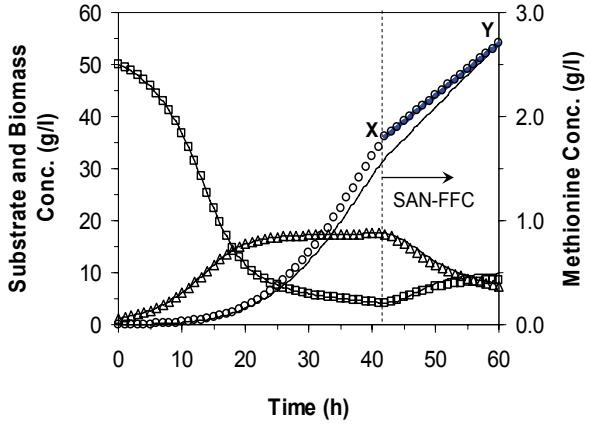

Figure 9: Performance of SAN-FFC strategy implementation in the absence of noise in the *DO* measurements. *XY* shows the desired trajectory. SAN-FFC forces the process is made to converge to the desired trajectory. (—); the symbols represent the ideal process dynamics (○ Methionine □ Substrate and Δ Biomass concentrations).

while Figure 12 shows the *DO* concentration with 5% noise and the control action as calculated from the SAN-FF control strategy. As in the previous case where no noise was present in the *DO* measurements, the process responds gradually to the SAN-FFC control action. The control objective is achieved before 60 h. The SAN exhibits a stable and robust prediction. Its adaptation to the changes in process is satisfactory. The performance SAN-feed forward controller shows a smooth control action. However, the accuracy in the prediction of SAN is reduced as indicated by the NRMSE values.

3.5 Performance of SAN-feed forward controller with random variation in process parameters

In the real process, the kinetics is changing continuously as the cells adapt to the changing environmental conditions. Although mechanistic models use constant parameters, a more accurate representation is achieved when the parameters are considered to be time varying. In this study, we consider those parameters that affect the specific growth rate because it is a sensitive parameter in methionine production. The specific growth rate μ, shows how the cell growth is regulated when the glucose, methionine and *DO* concentrations varying in

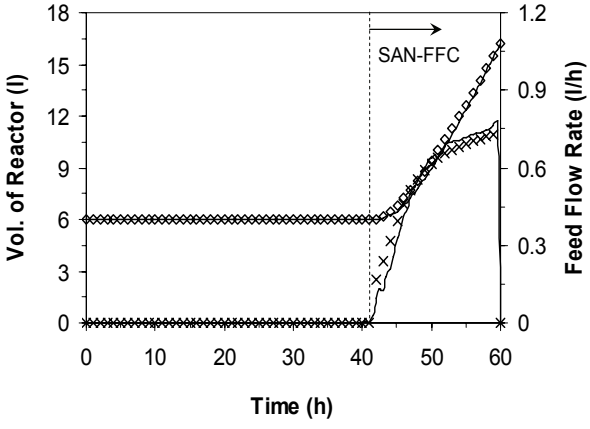

Figure 10: Control action of SAN-FFC in the absence of noise in *DO* measurements. The feed rate is computed from predicted values (—); the symbols represent the ideal process dynamics (× Substrate feed flow rate and ◊ volume of reactor).

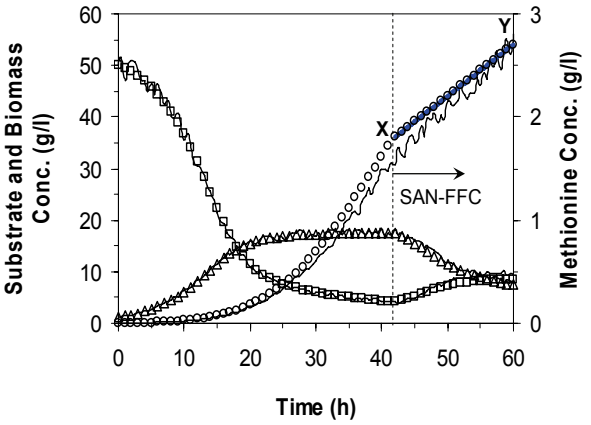

Figure 11: Performance of SAN-FFC strategy implementation when there is 5% noise in the *DO* measurements. *XY* shows the desired trajectory. SAN-FFC forces the process is made to converge to the desired trajectory. (—); the symbols represent the ideal process dynamics (○ Methionine □ Substrate and Δ Biomass concentrations)

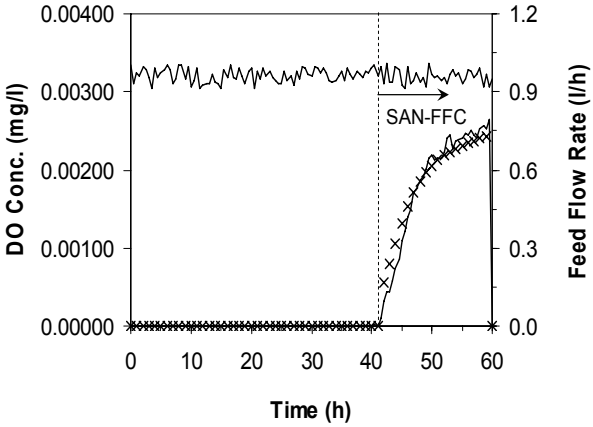

Figure 12: Control action of SAN-FFC when there is 5% noise in *DO* measurements. The feed rate is computed from predicted values (—); the symbols represent the ideal process dynamics (× Substrate feed flow rate and ◊ volume of reactor)

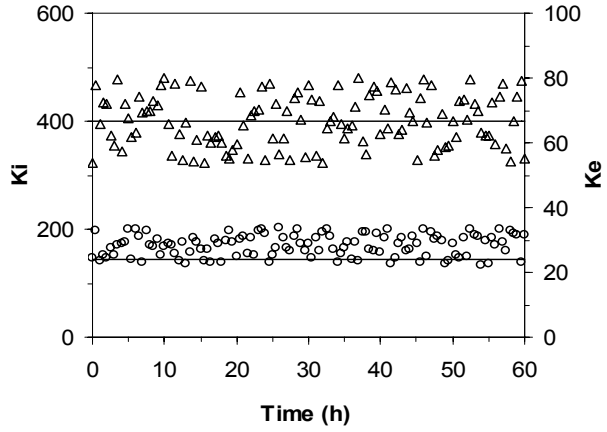

Figure 13: The parameters defining (K_e and K_i) the specific growth rate μ is varied randomly to account local mass-transfer gradients and local micro-aerobic conditions. (— mean value Δ K_i and ○ K_e)

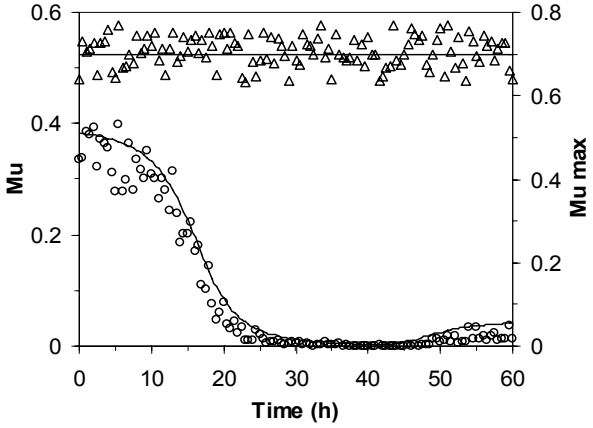

Figure 14: The specific growth rate μ varies randomly because of variations in. K_e and K_i (— mean value Δ μ_m and ○ μ)

the reactor. To reflect the changing conditions and challenge the SAN-feed forward controller, the parameters (μ_m, K_e and K_i) of equation (17) are randomly varied to get a reasonable degree of variation in μ. Random variations of parameters have been considered because the specific growth rate depends significantly on the micro-aerobic conditions of this process. Mixing patterns within the reactor will create local regions having different specific growth rates. The parameter variations and the resulting effect on μ are shown in Figs 13 and 14. The performance of the SAN-feed forward controller in this case is presented in Figs 15 and 16 and the NRMSE analysis is given in Table 2. The NRMSE results show that the total error in this case is lower than the previous case (with measurement noise) but higher than the ideal case (without measurement noise). The SAN-FFC performance shows robustness to parameter variations that is, changing process conditions.

Table 2: NRMSE analysis of Implementation Data Set (Without Noise, With Noise and Varying Model Parameter

Implementation Data Set	NRMSE					Total RMSE
	s	*x*	*p*	*V*	*F*	
Without Noise	8.8×10^{-4}	1.6×10^{-3}	3.2×10^{-3}	1.1×10^{-3}	3.1×10^{-3}	7.7×10^{-4}
With 5% Noise	1.5×10^{-3}	2.4×10^{-3}	5.3×10^{-3}	3.7×10^{-3}	5.1×10^{-3}	2.1×10^{-3}
With Varying Model Parameters	1.3×10^{-3}	1.8×10^{-3}	4.8×10^{-3}	2.65×10^{-3}	4.3×10^{-3}	9.4×10^{-4}

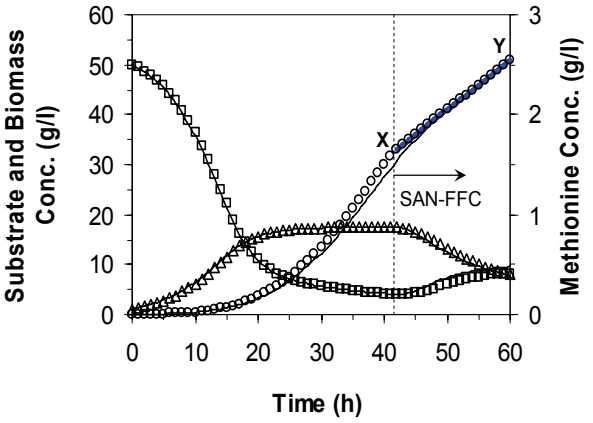

Figure 15: Performance of SAN-FFC strategy implementation when the specific growth rate μ is varied randomly; there is no noise in *DO* measurement. *XY* shows the desired trajectory. SAN-FFC converges quickly to the desired trajectory. (—); the symbols represent the ideal process dynamics (○ Methionine □ Substrate and Δ Biomass concentrations).

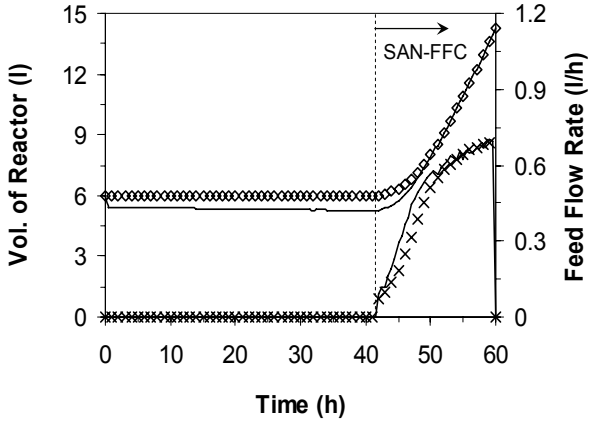

Figure 16: Control action of SAN-FFC when the specific growth rate μ is varied randomly; there is no noise in *DO* measurement. The feed rate is computed from predicted values (—); the symbols represent the ideal process dynamics (× Substrate feed flow rate and ◊ volume of reactor).

4. Conclusions

The performance of SAN-feed-forward controller in controlling methionine concentration along a predefined linear profile is satisfactory. The prediction of states by SAN is stable and robust. The NRMSE values increased for the noise in measurement and varying parameter case studies. However, the control action computed is smooth. The most important observation is that SAN adapts easily to process conditions for which it is not trained. It also meets the added challenge of performing in the presence of measurement noise and unknown time varying parameters. Further, the entire execution of the methionine production process is carried out using sampling intervals of 30 min to represent the difficult conditions that occur in the actual process more accurately. Under these stringent conditions SAN-feed forward controller executes one cycle of computation in average time of 15 sec. Our results demonstrate that SAN is good candidate for on-line implementation.

5. References

[1] J. S. Alford, "Bioprocess control: Advances and challenges", *Comp. Chem. Eng.*, Elsevier Sci., 30, 2006, pp. 1464-1475.

[2] P. F. Lith, B. H. L. Betlem, B. Roffel, "A structured modeling approach for dynamic hybrid fuzzy-first principle model", *J. Proc. Cont.*, Elsevier Sci., 12, 2002, pp. 605-615.

[3] J. Peres, R. Oliveira, S. F. Azevedo, "Knowledge based modular networks for process modeling and control", *Comp. Chem. Eng*., Elsevier Sci., 2001, 25, pp. 783-791.

[4] K. Schugerl, "Progress in monitoring, modeling and control of bioprocess during the last 20 years", *J. Biotech*, Elsevier Sci., 2001, 85, pp. 149-173.

[5] C. Komives, R. S. Parker, "Bioreactor state estimation and control", *Curt. Opin. Biotech*., Elsevier Sci., 2003, 14, pp. 468-474.

[6] R. Oliveira, "Combining First Principle Modeling and Artificial Neural Networks: A General Framework", *Comput. Chem. Eng.*, Elsevier Sci., 2004, 28, pp. 755-766.

[7] S. F. Azevedo, B. Dahm, R. Oliveira, "Hybrid Modeling of Biochemical Processes: A comparison with the conventional approach", *Comp. Chem. Eng*., Elsevier Sci., 1997, 21, pp. s751-s756.

[8] K. Gadkar, S. Mehra, J. Gomes, "On-line adaptation of neural networks for bioprocess control", *Comp. Chem. Eng*., Elsevier Sci., 2005, 29(5), pp. 1047-1057.

[9] J. Gomes, D. Kumar, "Production of L-methionine by submerged fermentation: A review", *Enz. Microbiol. Technol*., Elsevier Sci., 2005, 37(1), pp. 3-18.

[10] D. Kumar, S. Garg, V. S. Bisaria, T. R. Sreekrishnan, J. Gomes, "Production of methionine by a multi-analogue resistant mutant of *Corynebacterium lilium*", *Process Biochem*., Elsevier Sci., 2003, 38, pp. 1165-1171.

Appendix

Model Parameter	Description	Value
δ_1	Growth associated formation rate for all products and by-products	1.05×10^{-4}
δ_2	Non-growth associated formation rate for all products and by-products.	8.4×10^{-4}
$Y_{x/s}$	Biomass yield based on substrate	0.38
$Y_{p/s}$	Product yield based on substrate	0.105
$Y_{x/o}$	Biomass yield coefficient based on oxygen	2.33
$Y_{p/o}$	Product yield coefficient based on oxygen	3.26
s_c	Critical substrate concentration	3.25
ξ_1	$\left(1/Y_{x/s}+\delta_1/Y_{p/s}\right)$	2.633
ξ_2	$\left(\delta_2/Y_{p/s}\right)$	0.008
α	Non-growth associated product synthesis coefficient	0.0139
β	Growth associated product synthesis coefficient	0.00395
K_e	Exponential equivalent of the Monod constant	27.99
K_i	Substrate inhibition constant	400.26
$K_l a$	Mass transfer coefficient	50
c_l^*	Saturation value of dissolved oxygen concentration	0.008
κ	$\left(1/Y_{x/o}+\delta_1/Y_{p/o}\right)$	0.4292
λ	$\left(\delta_2/Y_{p/o}\right)$	0.000258
μ_m	Maximum specific growth rate	0.7